

DOI: 10.1002/cbic.200600117

# Organometallic Compounds with Biological Activity: A Very Selective and Highly Potent Cellular Inhibitor for Glycogen Synthase Kinase 3

G. Ekin Atilla-Gokcumen, Douglas S. Williams, Howard Bregman, Nicholas Pagano, and Eric Meggers\*<sup>[a]</sup>

*A chiral second-generation organoruthenium half-sandwich compound is disclosed that shows a remarkable selectivity and cellular potency for the inhibition of glycogen synthase kinase 3 (GSK-3). The selectivity was evaluated against a panel of 57 protein kinases, in which no other kinase was inhibited to the same extent, with a selectivity window of at least tenfold to more than 1000-fold at 100  $\mu$ M ATP. Furthermore, a comparison with organic GSK-3 inhibitors demonstrated the superior cellular activity of this ruthenium compound: wnt signaling was fully induced at concentrations down to 30 nM. For comparison, the well-established organic GSK-3 inhibitors 6-bromoindirubin-3'-oxime (BIO*

*and kenpaullone activate the wnt pathway at concentrations that are higher by around 30-fold and 100-fold, respectively. The treatment of zebrafish embryos with the organometallic inhibitor resulted in a phenotype that is typical for the inhibition of GSK-3. No phenotypic change was observed with the mirror-imaged ruthenium complex. The latter does not, in fact, show any of the pharmacological properties for the inhibition of GSK-3. Overall, these results demonstrate the potential usefulness of organometallic compounds as molecular probes in cultured cells and whole organisms.*

## Introduction

Chemical genetics has been conceived for an approach that uses small molecules as probes to study protein functions in cultured cells and whole organisms.<sup>[1]</sup> This area of research is focused almost entirely on the design of organic molecules. Our laboratory is instead interested in exploring inorganic and organometallic moieties as structural scaffolds for the design of biologically active compounds.<sup>[2–9]</sup> In this strategy, a metal center plays a structural role by organizing the organic ligands in the three-dimensional receptor space. We believe that this approach allows access to unexplored chemical space, thus giving new opportunities for the design of small molecules with unprecedented properties.<sup>[10]</sup>

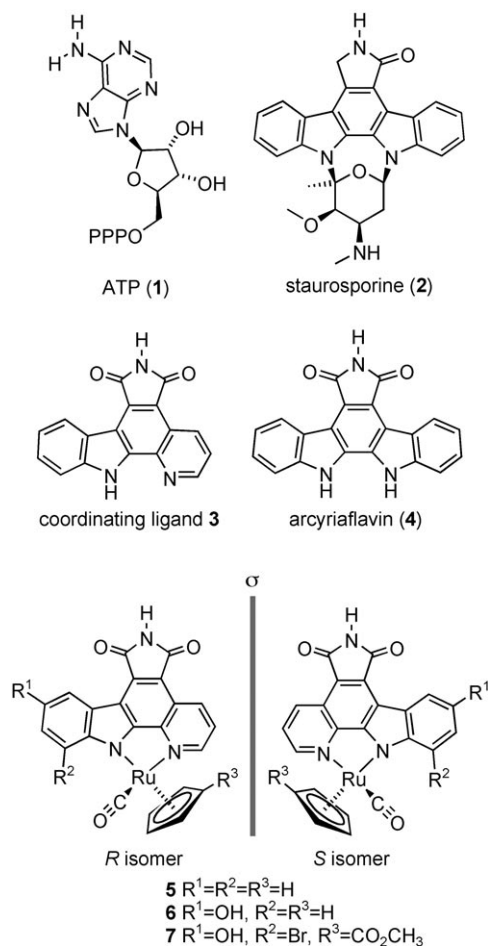
We initially designed metal complexes that can mimic more complicated natural products. For example, in order to match the overall shape of the ATP-binding site of protein kinases in a fashion similar to the ATP (1)-competitive staurosporine (2), but with less synthetic effort and more extended structural options, we replaced the indolocarbazole alkaloid scaffold with simple metal complexes in which the main features of the indolocarbazole aglycon are retained in the metal-chelating pyridocarbazole 3 (Scheme 1).<sup>[5–9]</sup> Ligand 3 is derived from arcyriaflavin A (4) by substituting one indole moiety for a pyridine. We established that ligand 3 can serve as a strong bidentate ligand for ruthenium and we discovered that the half-sandwich ruthenium complexes 5 and 6 are potent and ATP-competitive

inhibitors for glycogen synthase kinase 3 (GSK-3) and protein kinase Pim-1.<sup>[5,6,9]</sup> Compound 6 was also demonstrated to be active in human embryonic kidney cells, as well as in *Xenopus* embryos.<sup>[6]</sup> Compounds 5 and 6 are air-stable, stable in water, and can even withstand millimolar concentrations of thiols.

The real value of a molecular probe for chemical genetics depends on its specificity for the target protein. This is a formidable challenge in the area of designing protein kinase inhibitors, since the human genome codes for more than 500 individual members,<sup>[11]</sup> all of them displaying highly conserved ATP-binding sites.<sup>[12]</sup> Since the ATP-binding site is the most common target for the design of inhibitors, it is not surprising that many recent reexaminations of reportedly selective protein kinase inhibitors reveal that they in fact hit multiple kinases.<sup>[13,14]</sup>

[a] G. E. Atilla-Gokcumen, D. S. Williams, H. Bregman, N. Pagano, Prof. E. Meggers  
Department of Chemistry, University of Pennsylvania  
231 South 34th Street, Philadelphia, PA 19104 (USA)  
Fax: (+1) 215-746-0348  
E-mail: meggers@sas.upenn.edu

Supporting information for this article is available on the WWW under <http://www.chembiochem.org> or from the author: Structure–activity relationship with scaffold 5, cytotoxicity data, resolution of 7, and CD spectra.



**Scheme 1.** Designing ruthenium complexes as protein kinase inhibitors by using the ATP-competitive natural product staurosporine as a lead structure. The half-sandwich compounds 5–7 are pseudotetrahedral and exist in two mirror-imaged configurations. The absolute configuration at the ruthenium center has been assigned according to the priority order of the ligands being  $\eta^5\text{-C}_5\text{H}_5 > \text{pyridine} [\text{N}(\text{C}, \text{C}, \text{C})] > \text{indole} [\text{N}(\text{C}, \text{C}, \text{lone pair})] > \text{CO}$ .

We here demonstrate that organometallic compounds can fulfill the criteria for an exemplary molecular probe for protein kinases: high cellular potency and high target selectivity. We disclose the ruthenium complex (*R*)-7, which we obtained by performing a simple structure–activity relationship study. Organoruthenium compound (*R*)-7 is highly selective for GSK-3 in a panel of 57 different protein kinases. In addition, the compound has a subnanomolar binding constant for GSK-3 and is significantly more active in cell-based assays than some well-established organic GSK-3 inhibitors.

GSK-3 has been shown over the last several years to be a key component of a diverse range of cellular processes, for example, the signal transduction in the insulin and wnt signaling pathways.<sup>[15]</sup> Dysregulation of GSK-3 is linked to several diseases, such as diabetes, Alzheimer's disease, other neurodegenerative diseases, and cancer. Highly selective and cellular active pharmacological inhibitors of GSK-3 are therefore desired towards the goals of understanding the function of GSK-3 and the development of potential drug candidates.<sup>[16]</sup>

## Results and Discussion

### Selectivity profile of ruthenium complex 5

In order to evaluate the kinase selectivity of the initial half-sandwich scaffold 5, we profiled the racemate (*R,S*)-5 against a panel of 57 representative protein kinases. Table 1 shows the percentages of inhibition at 100 nM of (*R,S*)-5, or alternatively for some kinases, the concentration at which 50% of the protein kinase is inhibited ( $IC_{50}$ ). Most data points were measured at 100  $\mu\text{M}$  ATP, which is above the  $K_M$  of ATP for most of the tested kinases. Compound (*R,S*)-5 displays an  $IC_{50}$  for GSK-3 $\alpha$  of 20 nM and for GSK-3 $\beta$  of 50 nM (100  $\mu\text{M}$  ATP). For comparison, more than 50 of the kinases in the panel are not significantly inhibited at 100 nM of (*R,S*)-5. Interestingly, this includes the phylogenetically and structurally closely related cyclin-dependent kinases (CDKs), which show activities between 74 and 97% at 100 nM of (*R,S*)-5.<sup>[17]</sup> However, (*R,S*)-5 inhibits the protein kinase Pim-1 with an even higher potency ( $IC_{50}=3$  nM at 100  $\mu\text{M}$  ATP) than it does GSK-3 ( $\alpha$  and  $\beta$ ), and also inhibits the protein kinases MSK1 ( $IC_{50}=120$  nM, 100  $\mu\text{M}$  ATP), Rsk1 ( $IC_{50}=300$  nM, 100  $\mu\text{M}$  ATP), and TrkA ( $IC_{50}=70$  nM, 100  $\mu\text{M}$  ATP) to some considerable extent.

### Towards a selective GSK-3 inhibitor

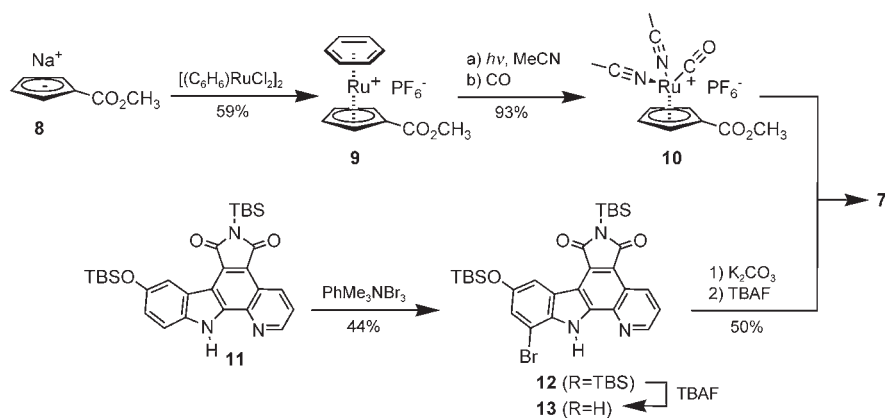
For a compound to be a truly useful molecular probe, the selectivity is a crucial parameter. Therefore, in an attempt to improve the selectivity profile for GSK-3, we performed a simple structure–activity relationship study starting by modifying the indole moiety and the cyclopentadienyl ligand of the half-sandwich scaffold 5. From a small random library of ten newly synthesized racemic compounds (see Supporting Information), we identified compound 7, having a hydroxyl group and bromine at the 5 and 7 positions of the indole, respectively, and a methyl ester at the cyclopentadienyl ligand, as the most selective derivative (Scheme 1). Compound 7 was synthesized as shown in Scheme 2. Accordingly, (methylcarbonyl)cyclopentadienyl sodium 8 was first treated with  $[\text{Ru}(\text{benzene})\text{Cl}_2]_2$  to provide sandwich complex 9 in 59% yield.<sup>[18]</sup> Compound 9 in acetonitrile was subsequently photolyzed with a medium-pressure mercury lamp; this resulted in the replacement of the benzene ligand by three acetonitriles, followed by the substitution of one acetonitrile by CO (9  $\rightarrow$  10, 93%).<sup>[19]</sup> Next, pyridocarbazole ligand 11<sup>[7]</sup> was brominated at the indole with phenyltrimethylammonium tribromide at room temperature to give 12 in 44% yield; this was followed by the reaction with 10 in the presence of  $\text{K}_2\text{CO}_3$ .<sup>[7]</sup> Removal of the TBS groups with TBAF yielded ruthenium complex 7 in 50% yield over two steps.

Half-sandwich compound 7 has metal-centered chirality. We resolved the racemic mixture of 7 with a ChiralPak AD-H analytical HPLC column (Daicel/Chiral Technologies).<sup>[20]</sup> The absolute configuration was assigned by correlation with the circular dichroism (CD) spectra of (*S*)-5 and (*R*)-6, both of which have recently been cocrystallized with the protein kinase Pim-1 (see Supporting Information).<sup>[9]</sup> In DMSO at room temperature, the enantiomers racemize with around 2% over 24 h, as deter-

**Table 1.** Protein kinase selectivity profile of the ruthenium complexes (*R,S*)-5 and (*R*)-7 against a panel of 57 protein kinases. The activities at 100 nM inhibitor or IC<sub>50</sub> values are displayed. Experiments were performed at 100 μM ATP unless indicated otherwise.

Kinases	( <i>R,S</i> )-5	( <i>R</i> )-7	Kinases	( <i>R,S</i> )-5	( <i>R</i> )-7
Abl	5 μM <sup>[b]</sup>	> 1 μM	IRAK4	77%	97%
ALK	87%	86%	JNK1α1	116%	102%
Arg	96%	105%	Lck	3 μM <sup>[b]</sup>	> 1 μM <sup>[a]</sup>
ASK1	98%	103%	Lyn	105%	97%
Aurora-A	102%	104%	MAPK1	93%	> 1 μM <sup>[a]</sup>
Bmx	84%	100%	MAPKAP-K2	94%	97%
CaMKII(r)	91%	97%	MEK1	99%	101%
CDK1/cyclin B	95%	99%	Met	126%	97%
CDK2/cyclin A	3 μM <sup>[b]</sup>	600 nM <sup>[a]</sup>	<b>MSK1</b>	<b>120 nM</b>	<b>3 μM<sup>[a]</sup></b>
CDK2/cyclin E	74%	53%	MSK2	82%	98%
CDK3/cyclin E	76%	96%	NEK6	104%	101%
CDK5/p35	79%	88%	PAK4	88%	85%
CDK6/cyclin D3	97%	90%	PDGFRα	107%	100%
CDK7/cyclin H	92%	99%	PDK1	93%	110%
CHK1	25 μM <sup>[b]</sup>	> 1 μM <sup>[a]</sup>	<b>Pim-1</b>	<b>3 nM</b>	<b>35 nM</b> <b>(25 nM)<sup>[c]</sup></b>
CHK2	77%	92%	PKA	99%	96%
CK1δ	96%	101%	PKBα	93%	93%
c-RAF	87%	78%	PKCα	100 μM <sup>[b]</sup>	> 1 μM <sup>[a]</sup>
CSK	105%	85%	PKCβII	97%	104%
c-Src	4 μM <sup>[b]</sup>	67%	PRAK	94%	105%
EGFR	81%	88%	ROCK-I	88%	99%
EphB2	130%	85%	Ros	86%	94%
EphB4	97%	93%	<b>Rsk1</b>	<b>300 nM</b>	<b>800 nM<sup>[a]</sup></b>
Fes	111%	85%	Rsk2	84%	80%
FGFR3	89%	94%	SAPK2a	103%	95%
Fyn	77%	72%	Syk	95%	96%
<b>GSK-3α</b>	<b>20 nM</b>	<b>0.35 nM</b> <b>(1.5 nM)<sup>[c]</sup></b>	<b>TrkA</b>	<b>70 nM</b>	<b>350 nM<sup>[a]</sup></b>
<b>GSK-3β</b>	<b>50 nM</b>	<b>0.55 nM</b> <b>(2 nM)<sup>[c]</sup></b>	ZAP-70	15 μM <sup>[b]</sup>	> 1 μM <sup>[a]</sup>
IKKα	97%	96%			

[a] Determined at 10 μM ATP. [b] Determined at 20 μM ATP. [c] Compounds were preincubated with the kinase in the presence of ATP for 1 h before initiation of the phosphorylation with the addition of MgCl<sub>2</sub> (30 mM) and [γ-<sup>32</sup>P]ATP.



**Scheme 2.** Synthesis of GSK-3 inhibitor 7.

mined by chiral HPLC. However, if stored in the freezer, DMSO solutions of the individual isomers are configurationally completely stable. Of the two enantiomers, only the *R* isomer displays the desired properties.

concentrations below 100 nM of (*R*)-7 (Table 1). In conclusion, in this panel of protein kinases, (*R*)-7 is highly selective for GSK-3. Thus, with (*R*)-7, we have succeeded in developing a highly selective GSK-3 inhibitor.

Compound (*R*)-7 displays low IC<sub>50</sub> values of 350 pM against the α-isoform of GSK-3 and 550 pM against the β-isoform at an ATP concentration of 100 μM. Importantly, the IC<sub>50</sub> for Pim-1 is 35 nM, thus satisfactory selectivity factors of 100 (with respect to GSK-3α) and 64 (with respect to GSK-3β) are reached. These data and all other data in Table 1 were obtained by a conventional radioactive assay, in which the phosphorylation event was measured by the degree of phosphorylation of a substrate with [γ-<sup>32</sup>P]ATP. In most cases, the protein kinase was first incubated with the inhibitor, then the phosphorylation event was initiated by the addition of ATP, along with [γ-<sup>32</sup>P]ATP. Interestingly, if the inhibitor (*R*)-7 is instead preincubated with the protein kinase in the presence of ATP (60 min) and the reaction then initiated by the addition of Mg<sup>2+</sup> ions, the IC<sub>50</sub> values of (*R*)-7 for GSK-3 increased to 1.5 nM and 2.0 nM for the α- and β-isoforms, respectively. We attribute this effect, which we have not observed with the weaker inhibitor (*R,S*)-5, to the slow off-rate of (*R*)-7 once bound to GSK-3. In any case, even under these conditions, (*R*)-7 still shows satisfactory selectivities for GSK-3 over Pim-1 of 17-fold (α-isoform) and 13-fold (β-isoform).

Tested against an extended panel of protein kinases (Table 1), (*R*)-7 also shows an improved selectivity against the other problematic protein kinases MSK1 (IC<sub>50</sub> = 3 μM, 10 μM ATP), Rsk1 (IC<sub>50</sub> = 800 nM, 10 μM ATP), and TrkA (IC<sub>50</sub> = 350 nM, 10 μM ATP), with selectivity factors of more than two orders of magnitude. All other kinases are not significantly inhibited at

It is noteworthy that the pyridocarbazole ligand **13** itself (synthesized by TBAF treatment of **12**, Scheme 2), devoid of the ruthenium, considerably prefers Pim-1 ( $IC_{50}=10$  nM,  $100 \mu\text{M}$  ATP) over GSK-3 ( $\alpha$ -isoform:  $IC_{50}>30$  nM,  $\beta$ -isoform:  $IC_{50}>50$  nM,  $100 \mu\text{M}$  ATP).<sup>[21]</sup> Consequently, the ruthenium half-sandwich fragment in (*R*)-**7** not only increases the potency for GSK-3 by more than an order of magnitude, but also reverses the kinase selectivity in favor of GSK-3 inhibition. It is also noteworthy that the stereochemistry of the ruthenium fragment plays a crucial role, as demonstrated with the  $IC_{50}$  curves in Figure 1. The mirror-image isomer (*S*)-**7** significantly prefers

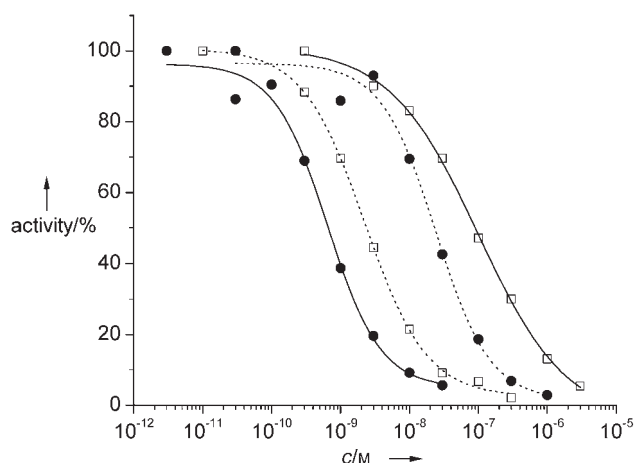


**Figure 1.**  $IC_{50}$  curves of the half-sandwich organometallics (*R*)-**7** (●) and (*S*)-**7** (□) against GSK-3 $\beta$  (—) and Pim-1 (---). See Experimental Section for details.

Pim-1 ( $IC_{50}=3$  nM,  $100 \mu\text{M}$  ATP) over GSK-3 ( $\alpha$ -isoform:  $IC_{50}=80$  nM,  $\beta$ -isoform:  $IC_{50}=90$  nM,  $100 \mu\text{M}$  ATP), thus leading to a complete switch in kinase selectivity.

### Cellular activity of (*R*)-**7**

We next investigated the cellular potency of (*R*)-**7** by probing the wnt signal-transduction pathway.<sup>[15]</sup> In this pathway, GSK-3 $\beta$  acts as a negative regulator by phosphorylating  $\beta$ -catenin. Phosphorylated  $\beta$ -catenin itself is unstable and is degraded rapidly by the proteasome. In the presence of a wnt signal, GSK-3 $\beta$  is inactivated, and this results in an accumulation of  $\beta$ -catenin in the cytoplasm, followed by a subsequent translocation into the nucleus where  $\beta$ -catenin serves as a transcriptional coactivator through its interaction with the T-cell factor (TCF) family of transcription factors (Figure 2). Thus inhibition of GSK-3 $\beta$  by pharmacological inhibitors or by wnt signaling leads to increased  $\beta$ -catenin levels and activation of wnt dependent transcription.

In order to determine the activation of the wnt pathway as a response to intracellular inhibition of GSK-3 $\beta$ , we used human embryonic kidney cells (HEK293OT) that have stably incorporated a Tcf-luciferase transcription reporter (OT-Luc cells).<sup>[22]</sup> This transcription reporter generates luciferase in response to increased concentrations of  $\beta$ -catenin. We incubated

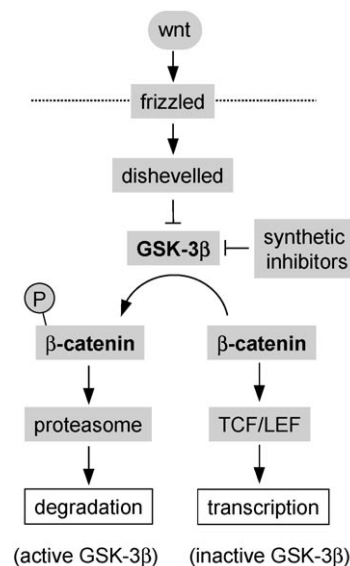


**Figure 2.** Wnt pathway: Inactivation of GSK-3 $\beta$  by a wnt signal or small-molecule inhibitor results in the transcription of target genes.

these OT-Luc cells with varying concentrations of compounds **5**, (*R*)-**7**, and the organic GSK-3 inhibitors kenpallone<sup>[23]</sup> and 6-bromoindirubin-3'-oxime (BIO)<sup>[24]</sup> for a period of 24 h. An upregulation of luciferase was determined by the luminescence signal upon addition of luciferin to the cell lysate. Intriguingly, (*R*)-**7** shows high activities at down to nanomolar concentrations. For example, at 30 nM, (*R*)-**7** displays almost complete activity with a luminescence increase by a factor of almost 700. No other tested compound could match this cellular activity: the initial ruthenium compound (*R,S*)-**5** and the organic inhibitors kenpallone and BIO need micromolar concentrations for significant activities (Figure 3).

We next analyzed the cellular  $\beta$ -catenin concentration by Western blotting after incubation with (*R*)-**7**. Figure 4 qualitatively demonstrates a clear increase in  $\beta$ -catenin even in the presence of only 30 nM (*R*)-**7**. To further verify the activation of the wnt pathway that results in the translocation of  $\beta$ -catenin into the nucleus, we performed  $\beta$ -catenin staining experiments in melanoma cells (1205Lu) after exposure to (*R*)-**7**.<sup>[25,26]</sup> For this, cells were fixed and incubated first with a primary antibody against  $\beta$ -catenin followed by a secondary Texas Red-conjugated antibody. Immunofluorescence microscopy demonstrated that most of the  $\beta$ -catenin was indeed located in the nuclei and that this effect was observed at low concentrations of only 30 nM (*R*)-**7** (Figure 5). Thus, these experiments unambiguously demonstrate that (*R*)-**7** activates the wnt pathway in cell culture at nanomolar concentrations.

It is notable that all the tested organic and organometallic GSK-3 inhibitors display a bell-shaped activity profile. Decreased expression of luciferase at higher concentrations of the kinase inhibitors might reflect cytotoxicity resulting from the complete inhibition of the ubiquitous kinase GSK-3.<sup>[27]</sup> In fact, incubation of HeLa cells with different concentrations of (*R,S*)-**5**, (*R*)-**7**, BIO, and kenpallone for a period of 24 h, followed by testing the cell viability with an MTT assay, confirmed

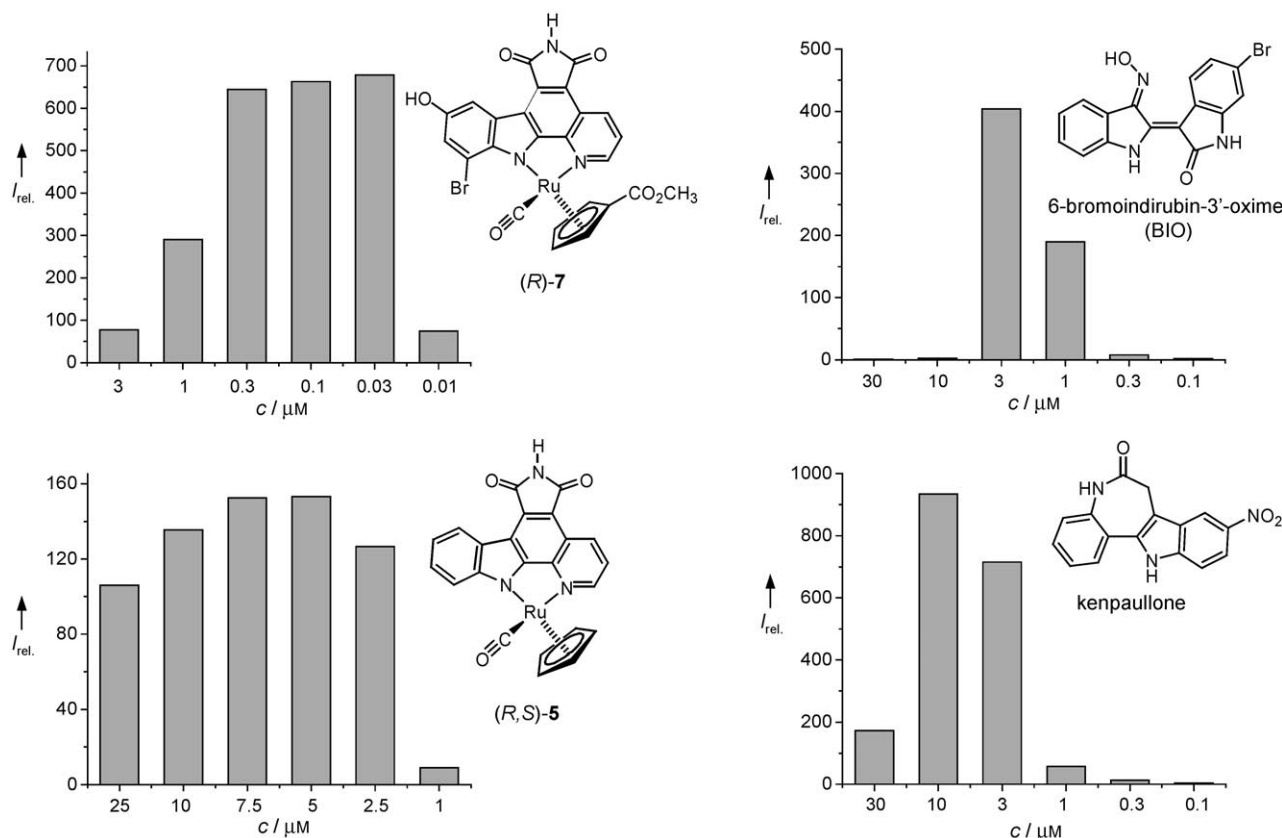


**Figure 3.** Cellular activities of ruthenium complexes *(R,S)*-5 and *(R)*-7, and comparison with organic GSK-3 inhibitors. Cells transfected with a  $\beta$ -catenin-responsive luciferase reporter were treated with different concentrations of *(R)*-7, *(R,S)*-5, BIO, or kenpaullone for 24 h. Luminescence signals were measured after cell lysis and the addition of luciferin.

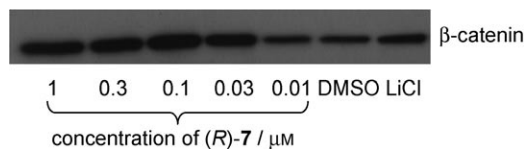


**Figure 4.** Qualitative detection of cellular concentrations of  $\beta$ -catenin as a function of incubation with *(R)*-7. DMSO (0.5%) and LiCl (30 mM) were used as negative and positive controls, respectively. The cells were incubated with the compounds for 24 h, and the concentration of  $\beta$ -catenin was verified by Western blotting. Each lane contains the same total amount of protein.

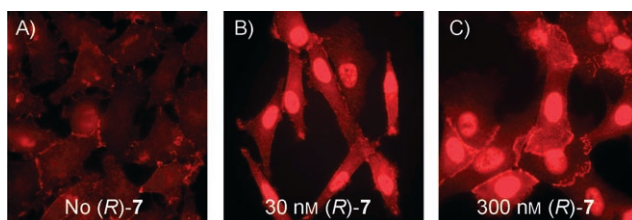


**Figure 5.** Cellular  $\beta$ -catenin staining in melanoma cells (1205 Lu) as a function of the concentration of *(R)*-7. The cells were seeded onto glass coverslips and incubated overnight in the presence of 0, 30, or 300 nM *(R)*-7. Cells were then fixed in 4% formaldehyde solution, permeabilized with Triton X-100, incubated with a primary antibody raised against  $\beta$ -catenin, and subsequently treated with an anti-mouse Texas Red-conjugated secondary antibody. Coverslips were then analyzed by immunofluorescence microscopy.

that both the organic and organometallic compounds are cytotoxic at higher concentrations (see Supporting Information for more details). This cytotoxicity correlates with the  $\text{IC}_{50}$  against GSK-3. Thus, the cytotoxicity might be directly related to the inhibition of GSK-3; however, the involvement of unidentified protein kinase targets cannot be excluded at this point.

### Zebrafish embryo phenotype

In order to demonstrate the utility of the organometallic reagent *(R)*-7 for experiments in entire organisms, we performed phenotypic experiments in zebrafish embryos. Wnt signaling, and thus GSK-3 $\beta$ , plays a crucial role in the development of metazoan.<sup>[28]</sup> For example, the exposure of zebrafish embryos at the four-hour stage to LiCl, a known GSK-3 inhibitor, promotes a perturbed development of the head structure with a no-eye phenotype, among others.<sup>[29]</sup> In order to test the activities of *(R)*-7 in zebrafish, we exposed the embryos to this compound at early stages of development. Accordingly, the embryos were collected and maintained in E3 media at 28.5 °C, and *(R)*-7 was added at 4 h post fertilization (hpf) to a final concentration of 1  $\mu\text{M}$ . When the phenotypes are compared at 25 hpf, reduced development of the anterior and posterior termini was observed. Treatment with *(R)*-7 results in a decrease of head structure without eyes and a stunted and crooked tail.

In addition, the yolk is enlarged and misshapen (Figure 6C). However, zebrafish embryos that were treated under identical conditions with (S)-7 develop completely normally (Figure 6A and B). Thus, these observations are consistent with an inhibition of GSK-3 by (R)-7, but not (S)-7.

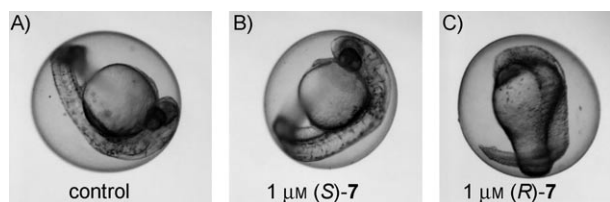


**Figure 6.** Exposure of zebrafish embryos to A) DMSO (2%), B) 1  $\mu\text{M}$  (S)-7, and C) 1  $\mu\text{M}$  (R)-7. The embryos were collected and maintained in E3 medium at 28.5 °C, compounds were added at 4 hpf, and the phenotypes were compared at 25 hpf.

## Conclusion

We have here demonstrated that metal-containing compounds are suitable as molecular probes in chemical genetics. In fact, as a molecular probe for the function of GSK-3, (R)-7 is superior to many reported organic GSK-3 inhibitors with respect to binding affinity, cellular potency, and kinase selectivity. It is likely that structures such as (R)-7 cannot be easily mimicked by an organic scaffold, and we are consequently accessing an area of chemical space that is unexplored or even inaccessible to organic compounds. Therefore, our approach of using organometallic scaffolds for the design of enzyme inhibitors promises to yield bioactive molecules with novel properties.

## Experimental Section

**General procedures and materials:** NMR spectra were recorded on a Bruker AM-500 (500 MHz) or DMX-360 (360 MHz) spectrometer. High-resolution mass spectra were obtained with a Micromass AutoSpec instrument by using either CI or ES ionization. Infrared spectra were recorded on a Perkin–Elmer 1600 series FTIR spectrometer. Solvents and reagents were used as supplied from Fisher, Sigma–Aldrich, Acros, or Strem (Newburyport, MA). The GSK-3 inhibitors BIO and kenpaullone were purchased from CalBioChem (La Jolla, CA). Reactions were performed under argon unless otherwise specified. TBS-protected pyridocarbazole **11** was synthesized as published recently.<sup>[7]</sup> Protein kinases (human) were purchased from Upstate (Charlottesville, VA). The substrate for TrkA was synthesized by Bachem (KKSPGEYVIEFG). All other substrates were purchased from Upstate.

**Kinase assays:** Percentage kinase activities at concentrations of 100 nM (R,S)-5 and (R)-7 were measured by Upstate (Kinase Profiler). The ATP concentration was 100  $\mu\text{M}$ .  $\text{IC}_{50}$  determinations with CDK2/cyclin A, GSK-3 $\alpha$ , GSK-3 $\beta$ , MSK1, Pim-1, and Rsk1: various concentrations of inhibitors were incubated at room temperature in MOPS (20 mM),  $\text{MgCl}_2$  (30 mM), bovine serum albumin (BSA; 0.8  $\mu\text{g mL}^{-1}$ ), DMSO (5%; resulting from the inhibitor stock solution), pH 7.0, in the presence of substrate (CDK2/cyclin A: 0.1  $\text{mg mL}^{-1}$  histone H1; GSK-3 $\alpha$  and GSK-3 $\beta$ : 20  $\mu\text{M}$  phosphoglycogen synthase kinase-2; MSK1: 30  $\mu\text{M}$  crosstide; Pim-1: 50  $\mu\text{M}$  S6 kinase/Rsk2 substrate peptide; Rsk1: 50  $\mu\text{M}$  MAPKAP kinase 2 sub-

strate) and kinase (CDK2/cyclin A: 0.08  $\text{ng mL}^{-1}$ ; GSK-3 $\alpha$  and GSK-3 $\beta$ : 0.0027  $\text{ng mL}^{-1}$  for (R)-7, 0.02  $\text{ng mL}^{-1}$  for (S)-7, 0.01  $\text{ng mL}^{-1}$  for (R,S)-5; MSK1: 0.04  $\text{ng mL}^{-1}$ ; Pim-1: 0.01  $\text{ng mL}^{-1}$ ; RSK1: 0.04  $\text{ng mL}^{-1}$ ). After 15 min, the reaction was initiated by adding ATP to the final concentrations indicated in Table 1, including [ $\gamma$ - $^{32}\text{P}$ ]ATP (ca. 0.2  $\mu\text{Ci mL}^{-1}$ ). Reactions were performed in a total volume of 25  $\mu\text{L}$ . After 60 min for (R,S)-5, or 120 min for (R)-7, the reactions were terminated by spotting 17.5  $\mu\text{L}$  onto a circular P81 phosphocellulose paper (diameter 2.1 cm, Whatman), followed by washing with 0.75% phosphoric acid (1 $\times$ ) and with acetone (4 $\times$ ). The dried P81 papers were transferred to a scintillation vial and scintillation cocktail (5 mL) was added. The counts per minute (CPM) were determined with a Beckmann 6000 scintillation counter.  $\text{IC}_{50}$  values were defined as the concentration of inhibitor at which the CPM was 50% of the control sample, corrected by the background.

**Assays with TrkA:** Assays were performed by following the same procedure as above, but in MOPS/NaOH (42 mM, pH 7.2), EDTA (1.1 mM), 0.5% glycerol, 0.001% Brij 35, 0.01%  $\beta$ -mercaptoethanol, and BSA (0.1  $\text{mg mL}^{-1}$ ) in the presence of substrate (100  $\mu\text{M}$ ) and TrkA (0.2  $\text{ng mL}^{-1}$ ). After 15 min, the reactions were initiated by adding ATP to the final concentrations indicated in Table 1, including [ $\gamma$ - $^{32}\text{P}$ ]ATP (ca. 0.2  $\mu\text{Ci mL}^{-1}$ ) and  $\text{MgCl}_2$  (final concentration of 25 mM).

**Alternative assay procedure** ( $\text{IC}_{50}$  values in brackets in Table 1): The same procedure as above was used, but the compounds were preincubated with the kinase, in the presence of ATP and peptide, in  $\text{MgCl}_2$ -free buffer. After a preincubation time of 1 h, the phosphorylation was started by the addition of  $\text{Mg}(\text{OAc})_2$  to a final concentration of 30 mM, and the addition of [ $\gamma$ - $^{32}\text{P}$ ]ATP (final concentration ca. 0.2  $\mu\text{Ci mL}^{-1}$ ).

**Luciferase assays:** Human embryonic kidney cells (HEK293T) with stably incorporated Tcf-luciferase transcription reporter (OT-Luc cells) were maintained in DMEM plus 10% fetal bovine serum (FBS) containing 1% penicillin/streptomycin at 37 °C under an atmosphere of 5%  $\text{CO}_2$  at constant humidity. Prior to the luciferase assay, cells were plated on six-well plates (ca.  $2.5 \times 10^5$  cells were grown in 2 mL culture media) and allowed to grow for 24 h. Thereafter, the medium was replaced by fresh medium (2 mL), and inhibitor solution (10  $\mu\text{L}$ , 200 times concentrated in 100% DMSO; LiCl was added as a sterile aqueous solution) was added. The cells were subsequently incubated with the inhibitors for 24 h. The medium was removed from each well, and each well was washed with phosphate buffered saline (PBS; 1 mL). The luciferase assay system (Promega) was used for lysing the cells and for the following luciferase assay. Cells were lysed by adding lysis buffer (200  $\mu\text{L}$ ) supplemented with protease inhibitor cocktail and phosphatase inhibitor cocktails I and II from Sigma. The lysis procedure was carried out on ice. The lysates were transferred to 500  $\mu\text{L}$  tubes, vortexed for 10–15 s, and left on ice for 20 min before being separated in a centrifuge at 10000 rpm and 4 °C for 10 min. Supernatants were transferred into different tubes and stored at  $-80$  °C. For the luciferase assay, the substrate was dissolved in buffer (both provided in the kit) according to the manufacturer's protocol. Luciferase assay substrate (100  $\mu\text{L}$ ) was added to the cell lysate (10  $\mu\text{L}$ ), and the luminescence signal was measured immediately by using a Monolight 3010 Luminometer from BD Biosciences.

**Western blotting:** The lysates obtained for the luciferase assays were used for Western blots. Each lane of the protein gel was loaded with the same amount of protein (14  $\mu\text{g}$  total), based on the concentration values determined by a Bradford assay. The protein gel contents were transferred to a nitrocellulose membrane,

which was immunoblotted for  $\beta$ -catenin and  $\beta$ -tubulin as a loading control.

**$\beta$ -Catenin fluorescence staining experiments:** Melanoma cells (1205Lu) were seeded onto glass coverslips in six-well plates and incubated overnight in 2% tumor medium (MCDB153/L15 4:1, supplemented with 2 mM  $\text{CaCl}_2$ ), heat-inactivated FBS (2%), and insulin ( $5 \mu\text{g mL}^{-1}$ ) at  $37^\circ\text{C}$  under an atmosphere of 5%  $\text{CO}_2$  at constant humidity. Cells were then fixed in 4% formaldehyde solution (Electron Microscopy Systems, Hatfield, PA) and permeabilized with Triton X-100 (0.2% v/v) before being blocked in PBS containing 1% BSA. Coverslips were incubated with a primary antibody raised against  $\beta$ -catenin (1:50; BD Pharmingen, San Diego, CA) at  $37^\circ\text{C}$  in a humidified atmosphere for 1 h. Coverslips were then washed in PBS (3 $\times$ ) before being incubated with an anti-mouse Texas Red-conjugated secondary antibody (Vector Laboratories, Burlingame, CA) for 1 h under similar conditions to those used for the primary antibody (dilution factor of 1:250). Coverslips were then further washed in PBS and sterile water before being treated with VectorShield anti-fade and analyzed by immunofluorescence microscopy.

**Compound 9:** Compound **8** (58.4 mg, 0.4 mmol), synthesized from cyclopentadienyl sodium and dimethylcarbonate,<sup>[30]</sup> and  $[\text{Ru}(\text{benzene})\text{Cl}_2]_2$  (100 mg, 0.2 mmol) in acetonitrile (10 mL) were heated under reflux overnight under argon. The resulting suspension was filtered through celite and evaporated to result in a yellow oil, which was dissolved in MeOH and precipitated as hexafluorophosphate salt upon addition of ammonium hexafluorophosphate. The resulting pale yellow solid was collected by filtration, washed with cold water, and dried under high vacuum. Yield: 106 mg (59%);  $^1\text{H NMR}$  (360 MHz,  $\text{CD}_3\text{CN}$ ):  $\delta = 6.16$  (s, 6H), 5.78 (m, 2H), 5.46 (m, 2H), 3.81 ppm (s, 3H);  $^{13}\text{C NMR}$  (90 MHz,  $\text{CD}_3\text{CN}$ ):  $\delta = 166.3, 88.5, 86.5, 83.3, 81.9, 53.7$  ppm; IR (thin film):  $\tilde{\nu} = 3129, 3102, 1725, 1474, 1435, 1399, 1372, 1290, 1202, 1152, 964, 829$   $\text{cm}^{-1}$ ; HRMS calculated for  $\text{C}_{13}\text{H}_{13}\text{O}_2\text{Ru}$ : 302.9959  $[\text{M}-\text{PF}_6]^+$ , found 302.9947  $[\text{M}-\text{PF}_6]^+$ .

**Compound 10:** A solution of compound **9** (100 mg, 0.2 mmol) in acetonitrile (225 mL) was irradiated with a medium-pressure mercury lamp through a uranium filter for 4.5 h while argon was bubbled through the solution. The solution was then concentrated to 10 mL, purged with  $\text{CO}$ , and left overnight under positive  $\text{CO}$  pressure. The resulting solution was evaporated and dried under high vacuum to give **10** as a yellow-brown oil (97 mg, 93%).  $^1\text{H NMR}$  (500 MHz,  $\text{CD}_3\text{CN}$ ):  $\delta = 5.84$  (m, 2H), 5.19 (m, 2H), 3.79 (s, 3H), 2.39 ppm (s, 6H);  $^{13}\text{C NMR}$  (75 MHz,  $\text{CD}_3\text{CN}$ ):  $\delta = 197.8, 166.2, 130.6, 90.2, 81.6, 80.4, 53.3, 4.4$  ppm; IR (thin film):  $\tilde{\nu} = 3124, 3011, 2959, 2014$  (CO), 1731, 1473, 1434, 1366, 1292, 1193, 1151, 1038, 961, 842, 773  $\text{cm}^{-1}$ ; ES-MS: 335  $[\text{M}-\text{PF}_6]^+$ .

**Compound 12:** Solid phenyltrimethylammonium tribromide (177 mg, 0.47 mmol) was added to a solution of **11** (50 mg, 0.094 mmol) in  $\text{CH}_2\text{Cl}_2$  (5 mL). The resulting orange solution was stirred at room temperature overnight. The solvent was then evaporated, and the crude material was purified by silica gel chromatography, elution with hexanes/ethyl acetate (10:1). The desired product was isolated as a yellow-orange solid (26 mg, 44%).  $^1\text{H NMR}$  (500 MHz,  $\text{CDCl}_3$ ):  $\delta = 10.18$  (brs, 1H), 9.42 (dd,  $J = 8.5, 1.3$  Hz, 1H), 9.00 (dd,  $J = 4.2, 1.6$  Hz, 1H), 8.73 (s, 1H), 7.80 (s, 1H), 7.66 (dd,  $J = 8.5, 4.3$  Hz, 1H), 1.14 (s, 9H), 1.08 (s, 9H), 0.64 (s, 6H), 0.41 ppm (s, 6H);  $^{13}\text{C NMR}$  (90 MHz,  $\text{CDCl}_3$ ):  $\delta = 175.3, 173.9, 148.9, 148.1, 139.3, 136.5, 135.2, 131.2, 122.9, 122.4, 122.3, 120.6, 117.1, 116.1, 115.8, 114.5, 113.3, 26.7, 26.2, 19.3, 18.7, -3.9, -4.2$  ppm; IR (thin film):  $\tilde{\nu} = 2955, 2930, 2858, 1750, 1695, 1528, 1463, 1335, 1306, 1257, 1225, 1185, 1127, 1069, 1048, 1011, 881$   $\text{cm}^{-1}$ ; HRMS

calcd for  $\text{C}_{29}\text{H}_{37}\text{N}_3\text{O}_3\text{Si}_2\text{Br}$ : 610.1557  $[\text{M}+\text{H}]^+$ , found 610.1579  $[\text{M}+\text{H}]^+$ .

**Compound 7:** A suspension of **12** (18.5 mg, 0.039 mmol), **10** (16.2 mg, 0.039 mmol), and potassium carbonate (5.3 mg, 0.039 mmol) in acetonitrile/methanol (2:1, 2.4 mL) was purged with argon for 15 min. The suspension was then stirred under argon overnight at room temperature during which time a color change from yellow to red/purple was observed. Tetrabutylammonium fluoride (1 M in THF, 193  $\mu\text{L}$ , 0.193 mmol) was added, and the solution was stirred for 15 min. Glacial acetic acid (3.3  $\mu\text{L}$ , 0.058 mmol) was added to the resulting solution. This mixture was stirred for additional 15 min, after which time the solvent was removed in vacuo. The crude material was dissolved in a minimal amount of  $\text{CH}_2\text{Cl}_2$  and subjected to silica gel chromatography (hexanes/ethyl acetate 2:1). Compound **7** was obtained as a pink/purple solid (13 mg, 50%).  $^1\text{H NMR}$  (360 MHz,  $[\text{D}_6]\text{DMSO}$ ):  $\delta = 11.09$  (s, 1H), 9.99 (s, 1H), 9.14 (d,  $J = 5.2$  Hz, 1H), 9.08 (d,  $J = 8.4$  Hz, 1H), 8.30 (s, 1H), 7.77 (dd,  $J = 8.4, 5.2$  Hz, 1H), 7.69 (s, 1H), 6.23 (m, 1H), 6.15 (m, 1H), 5.72 (m, 1H), 5.65 (m, 1H), 3.61 ppm (s, 3H);  $^{13}\text{C NMR}$  (125 MHz,  $[\text{D}_6]\text{DMSO}$ ):  $\delta = 199.4, 170.6, 170.5, 166.2, 155.7, 154.3, 147.8, 147.2, 143.9, 133.6, 131.1, 123.3, 121.3, 118.6, 113.9, 112.3, 110.5, 108.9, 90.6, 88.8, 82.4, 81.1, 77.0, 52.0, 45.8$ ; IR (thin film):  $\tilde{\nu} = 3415, 3273, 1968$  (CO), 1752, 1718, 1701, 1585, 1438, 1343, 1290, 1190, 1143, 1014, 843  $\text{cm}^{-1}$ ; HRMS calcd for  $\text{C}_{25}\text{H}_{15}\text{N}_3\text{O}_6\text{BrRu}$ : 633.9188  $[\text{M}+\text{H}]^+$ , found 633.9174  $[\text{M}+\text{H}]^+$ .

## Acknowledgements

We thank the University of Pennsylvania and the National Institutes of Health (1 R01 GM071695-01A1) for financial support of this research. We are also grateful for support from the laboratories of Dr. Michael A. Pack (University of Pennsylvania) regarding zebrafish experiments and Dr. Keiran S. M. Smalley (Wistar Institute, Philadelphia) regarding  $\beta$ -catenin-staining experiments in melanoma cells.

**Keywords:** glycogen synthase kinase 3 • medicinal chemistry • organometallic compounds • protein kinases • ruthenium


- [1] For chemical genetics, see: a) S. L. Schreiber, *Bioorg. Med. Chem.* **1998**, *6*, 1127–1152; b) T. U. Mayer, *Trends Cell Biol.* **2003**, *13*, 270–277; c) I. Smukste, B. R. Stockwell, *Annu. Rev. Genomics Hum. Genet.* **2005**, *6*, 261–286.
- [2] For metal-based drugs, see: a) C. Orvig, M. J. Abrams, *Chem. Rev.* **1999**, *99*, 2201–2842; b) Z. Guo, P. J. Sadler, *Angew. Chem.* **1999**, *111*, 1610–1630; *Angew. Chem. Int. Ed.* **1999**, *38*, 1512–1531; c) N. Farrell, *Coord. Chem. Rev.* **2002**, *232*, 1–230; d) I. Ott, B. Kircher, R. Gust, *J. Inorg. Biochem.* **2004**, *98*, 485–489; e) C. S. Allardyce, A. Dorcier, C. Scolaro, P. J. Dyson, *Appl. Organomet. Chem.* **2005**, *19*, 1–10; f) P. J. Dyson, G. Sava, *Dalton Trans.* **2006**, 1929–1933; g) U. Schatzschneider, N. Metzler-Nolte, *Angew. Chem.* **2006**, *118*, 1534–1537; *Angew. Chem. Int. Ed.* **2006**, *45*, 1504–1507.
- [3] For metal complexes as enzyme inhibitors, see: A. Y. Louie, T. J. Meade, *Chem. Rev.* **1999**, *99*, 2711–2734.
- [4] For bioorganometallic chemistry, see: a) K. Severin, R. Bergs, W. Beck, *Angew. Chem.* **1998**, *110*, 1722–1734; *Angew. Chem. Int. Ed.* **1998**, *37*, 1634–1654; b) D. B. Grotjahn, *Coord. Chem. Rev.* **1999**, *190*, 1125–1141; c) G. Jaouen (Ed.), *J. Organomet. Chem.* **1999**, *589*, 1–126; d) N. Metzler-Nolte, *Angew. Chem.* **2001**, *113*, 1072–1076; *Angew. Chem. Int. Ed.* **2001**, *40*, 1040–1043; e) R. H. Fish, G. Jaouen, *Organometallics* **2003**, *22*, 2166–2177; f) R. Stodt, S. Gencaslan, I. M. Müller, W. S. Sheldrick, *Eur. J. Inorg. Chem.* **2003**, 1873–1882; g) D. Schlawe, A. Majdalani, J. Velcicky, E. Heßler, T. Wieder, A. Prokop, H.-G. Schmalz, *Angew. Chem.* **2004**, *116*,

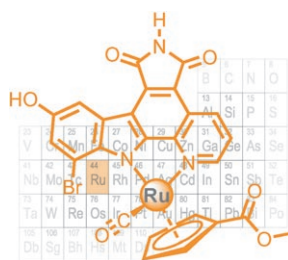
- 1763–1766; *Angew. Chem. Int. Ed.* **2004**, *43*, 1731–1734; h) D. R. Van Staveren, N. Metzler-Nolte, *Chem. Rev.* **2004**, *104*, 5931–5985; i) *Bioorganometallics* (Ed.: G. Jaouen), Wiley-VCH, Weinheim, **2005**.
- [5] H. Bregman, D. S. Williams, G. E. Atilla, P. J. Carroll, E. Meggers, *J. Am. Chem. Soc.* **2004**, *126*, 13594–13595.
- [6] D. S. Williams, G. E. Atilla, H. Bregman, A. Arzoumanian, P. S. Klein, E. Meggers, *Angew. Chem.* **2005**, *117*, 2020–2023; *Angew. Chem. Int. Ed.* **2005**, *44*, 1984–1987.
- [7] H. Bregman, D. S. Williams, E. Meggers, *Synthesis* **2005**, 1521–1527.
- [8] H. Bregman, P. J. Carroll, E. Meggers, *J. Am. Chem. Soc.* **2006**, *128*, 877–884.
- [9] J. É. Debreczeni, A. N. Bullock, G. E. Atilla, D. S. Williams, H. Bregman, S. Knapp, E. Meggers, *Angew. Chem.* **2006**, *118*, 1610–1615; *Angew. Chem. Int. Ed.* **2006**, *45*, 1580–1585.
- [10] For chemical space, see: C. M. Dobson, *Nature* **2004**, *432*, 824–828.
- [11] G. Manning, D. B. Whyte, R. Martinez, T. Hunter, S. Sudarsanam, *Science* **2002**, *298*, 1912–1934.
- [12] a) S. R. Hubbard, J. H. Till, *Annu. Rev. Biochem.* **2000**, *69*, 373–398; b) M. Huse, J. Kuriyan, *Cell* **2002**, *109*, 275–282.
- [13] For protein kinase inhibitor scaffolds, see: a) C. García-Echeverría, P. Traxler, D. B. Evans, *Med. Res. Rev.* **2000**, *20*, 28–57; b) A. J. Bridges, *Chem. Rev.* **2001**, *101*, 2541–2571.
- [14] For protein kinase inhibitor selectivities, see: a) S. P. Davies, H. Reddy, M. Caivano, P. Cohen, *Biochem. J.* **2000**, *351*, 95–105; b) J. Bain, H. McLauchlan, M. Elliott, P. Cohen, *Biochem. J.* **2003**, *371*, 199–204; c) M. A. Fabian, W. H. Biggs III, D. K. Treiber, *Nat. Biotechnol.* **2005**, *23*, 329–336; d) Z. A. Knight, K. M. Shokat, *Chem. Biol.* **2005**, *12*, 621–637.
- [15] a) P. J. Morin, *BioEssays* **1999**, *21*, 1021–1030; b) P. Cohen, S. Frame, *Nat. Rev. Mol. Cell Biol.* **2001**, *2*, 769–776; c) R. S. Jope, G. V. W. Johnson, *Trends Biochem. Sci.* **2004**, *29*, 95–102.
- [16] For a review on potent small organic inhibitors of GSK-3, see: A. Martinez, A. Castro, I. Dorronsoro, M. Alonso, *Med. Res. Rev.* **2002**, *22*, 373–384.
- [17] For cyclin dependent kinases, see: a) M. Knockaert, P. Greengard, L. Meijer, *Trends Pharmacol. Sci.* **2002**, *23*, 417–425; b) A. Huwe, R. Mazitschek, A. Giannis, *Angew. Chem.* **2003**, *115*, 2170–2187; *Angew. Chem. Int. Ed.* **2003**, *42*, 2122–2138.
- [18] B. M. Trost, C. M. Older, *Organometallics* **2002**, *21*, 2544–2546.
- [19] T. P. Gill, K. R. Mann, *Organometallics* **1982**, *1*, 485–488.
- [20] For optically active organometallic compounds, see: H. Brunner, *Angew. Chem.* **1999**, *111*, 1248–1263; *Angew. Chem. Int. Ed.* **1999**, *38*, 1194–1208.
- [21] The pyridocarbazole ligand **13** has a very low solubility that prevents a reliable determination of IC<sub>50</sub> values against the isoforms of GSK-3. Typically, the introduction of a metal fragment significantly improves the solubility in water/DMSO mixtures.
- [22] F. Zhang, C. J. Phiel, L. Spece, N. Gurchich, P. S. Klein, *J. Biol. Chem.* **2003**, *278*, 33067–33077.
- [23] M. Leost, C. Schultz, A. Link, Y. Wu, *Eur. J. Biochem.* **2000**, *267*, 5983–5994.
- [24] L. Meijer, A.-L. Skaltsounis, P. Magiatis, P. Polychronopoulos, M. Knockaert, M. Leost, X. P. Ryan, C. A. Vonica, A. Brivanlou, R. Dajani, C. Crovace, C. Tarricone, A. Musacchio, S. M. Roe, L. Pearl, P. Greengard, *Chem. Biol.* **2003**, *10*, 1255–1266.
- [25] K. Satyamoorthy, E. DeJesus, A. J. Linnenbach, B. Kraj, D. L. Kornreich, S. Rendle, D. E. Elder, M. Herlyn, *Melanoma Res.* **1997**, *7*, 35–42.
- [26] K. S. M. Smalley, P. Bradford, N. K. Haass, J. M. Brandner, E. Brown, M. Heryln, *Am. J. Pathol.* **2005**, *166*, 1541–1554.
- [27] J. Tan, L. Zhuang, H.-S. Leong, N. G. Iyer, E. T. Liu, Q. Yu, *Cancer Res.* **2005**, *65*, 9012–9020.
- [28] R. DasGupta, A. Kaykas, R. T. Moon, N. Perrimon, *Science* **2005**, *308*, 826–833.
- [29] a) S. E. Stachel, D. J. Grunwald, P. Z. Myers, *Development* **1993**, *117*, 1261–1274; b) W. Driever, *Curr. Opin. Genet. Dev.* **1995**, *5*, 610–618; c) S. van de Water, M. van de Wetering, J. Joore, J. Esseling, R. Bink, H. Clevers, D. Zivkovic, *Development* **2001**, *128*, 3877–3888.
- [30] W. P. Hart, D. Shihua, M. D. Rausch, *J. Organomet. Chem.* **1985**, *282*, 111–121.

Received: March 27, 2006

Published online on ■ ■ ■, 2006

## ARTICLES

 **A very picky organoruthenium inhibitor.** The shown enantiomerically pure ruthenium half-sandwich compound has been identified as a highly selective inhibitor for glycogen synthase kinase 3 (GSK-3) in a panel of 57 protein kinases. In addition, this compound displays a superior cellular activity compared to some organic GSK-3 inhibitors; this indicates that organometallic compounds can be attractive tools in chemical biology.



*G. E. Atilla-Gokcumen, D. S. Williams, H. Bregman, N. Pagano, E. Meggers\**



**Organometallic Compounds with Biological Activity: A Very Selective and Highly Potent Cellular Inhibitor for Glycogen Synthase Kinase 3**